The Astrophysical Journal, 592:1241–1251, 2003 August 1

CHARACTERISTICS OF SCATTER-FREE BEHAVIOR OF HELIOSPHERIC PICKUP IONS

J. G. Luhmann
University of California, Space Sciences Laboratory, Berkeley, CA 94720-7450; jgluhman@ssl.berkeley.edu
Received 2003 January 7; accepted 2003 April 8

ABSTRACT

Theoretical analyses of the global heliospheric pickup ion population generally involve the solution of forms of the Boltzmann or transport equation. Like their cosmic-ray counterparts, these approaches often presume a simplified geometry for the interplanetary magnetic field and that diffusive processes dominate the already picked up particles' behavior. At the opposite extreme lies the test particle picture of pickup ions, wherein their motion is tracked from the birth of the ions through their outward travel in the Parker spiral magnetic field. This approach has the advantage that it can include details of the source distribution, the initial pickup by the solar wind convection electric field at the site of ion production, and the combined effects of the radially evolving electric and magnetic fields experienced by the ions. Here test particles representing O^+ pickup ions are used to examine the influences of the source characteristics, including the heliocentric radius of their birth and the velocities of their parent neutrals. The consequences for ion populations from interstellar, interplanetary dust, and Jovian sources are considered. The results suggest some potentially observable features of general pickup ion distributions that could aid in the interpretation of their different sources.

Subject heading: interplanetary medium

1. INTRODUCTION

Heliospheric pickup ions result from the numerous sources that introduce neutral particles into the solar wind, including the interstellar gas that flows in at ~20–25 km s^{-1} relative to the Sun's frame of reference, interplanetary solids such as dust and asteroids that are sputtered by photons or particles from the Sun, and planets or comets that undergo various forms of outgassing and atmospheric escape (e.g., see the review by Kallenbach et al. 2000 and references therein). These sources supply atoms and molecules in a wide range of species, with characteristic initial velocities and spatial distributions. Photoionization, charge exchange with solar wind protons, or impact ionization by solar wind electrons ionizes the neutrals, which are then accelerated or "picked up" by the solar wind convection electric field $\boldsymbol{E} = -\boldsymbol{V}_{sw} \times \boldsymbol{B}$ (where $\boldsymbol{V}_{sw}$ is the solar wind velocity and $\boldsymbol{B}$ is the interplanetary magnetic field).

Heliospheric pickup ions have now been observed on AMPTE (Mobius et al. 1985), on the cometary missions *ICE*, *Giotto*, and *Sakigake* (Neugebauer 1990 and references therein), on *Ulysses* and *ACE* (Gloeckler et al. 2000), and on the *Cassini* spacecraft (Krimigis et al. 2002), using instruments in some cases sensitive to both ion mass and charge state operating in the energy range below several 100 keV. Some of the pickup ions have been linked to planetary sources, including Jupiter (Krimigis et al. 2002). The Jupiter source is interesting in that some of the neutrals escaping this gas giant are first accelerated to escape velocities as Io torus ions by Jupiter's corotation electric field and then reneutralized by charge exchange in the neutral torus, before they escape into the heliosphere (Barbosa, Eviatar, & Siscoe 1984). These have the distinction of having experienced a two-stage pickup process: one magnetospheric and one heliospheric. Another source process at Jupiter (and in other magnetospheres) is charge exchange of energetic trapped ions with the ambient neutrals, producing energetic neutral atoms at the trapped particle energies (e.g., Krimigis et al. 2002).

The traditional approach to theoretically analyzing the heliospheric behavior of pickup ions involves solutions of the Boltzmann or related transport equations for their distribution functions, as for cosmic rays but with in situ sources. This generally requires restrictive assumptions concerning the interplanetary magnetic field configuration, scattering/diffusion terms, and particle anisotropies and gyrotropies (e.g., Vasyliunas & Siscoe 1976; Fichtner et al. 1996; Isenberg 1997; Lu & Zank 2001). For example, an azimuthal interplanetary field might be adopted and anisotropies neglected under the assumption that the ions are produced in the outer heliosphere and that scattering rapidly distributes them over all pitch angles. However, analyses of pickup ion observations (e.g., Gloeckler, Fisk, & Schwadron 1995) suggest that some ion production occurs in the inner heliosphere and that at least out to the distance of Jupiter's orbit scattering mean free paths may be ~AU. Pickup ion distributions in the inner heliosphere might be expected to retain their original ring distributions because they are energetically unimportant compared to the much larger ambient particle contributions in this spatial domain. They are thus not likely to be strongly scattered by self-generated waves and are effectively a test particle population. Moreover, they should exhibit practically gyrotropic distributions because their sources have spatial gradients much larger than an ion gyroradius.

In a few contrasting theoretical studies of solar energetic particles from flares, Giacalone, Jokipii, & Mazur (2000) used test particle methods to demonstrate that structure in the observed time series of these proton fluxes could result from simple transport from a localized source, along a braided Parker spiral magnetic field created by footpoint motions on the rotating Sun. Test particle methods are also appropriate in such applications where the densities of the particles under study are insufficient for mutually collective behavior and in cases where collisions or other diffusive processes (e.g., scattering by wave-particle interactions) are not a dominant influence. In particular, in the high-energy fringes of a distribution, or for weakly or noninteracting

minor ion species, test particle descriptions can lend unique and useful insights into the behavior imposed by prescribed force fields and source and loss processes. These should have significant effects on the pickup ion distributions under consideration even in the presence of weak to moderate scattering.

Here test particle calculations in a radially flowing solar wind with a Parker spiral magnetic field are applied to learn more about heliospheric pickup ion behavior for the different types of sources. It is demonstrated how the test particle approach allows investigation of pickup ion distributions—spatial, velocity, and directional—from sources having virtually any form or character. Singly ionized oxygen atoms are selected as the example for study because this species arises from all of the above-mentioned sources and because the pickup ion trajectories are essentially mass-independent, except for source and ionization effects on the ions' initial locations and velocities. The results suggest some observable features of pickup ion distributions that could be used to more fully diagnose their sources.

2. APPROACH

The basic calculation in test particle approaches is the solution of the equation of motion, which gives the particles' positions and velocities as a function of time. Modern workstations easily handle numerical integrations of the ion equation of motion, including solar gravity and the Lorentz force $q(\boldsymbol{E} + \boldsymbol{v} \times \boldsymbol{B})$, where q is the ion charge, $\boldsymbol{v}$ is the ion velocity, and $\boldsymbol{E} = -\boldsymbol{V}_{sw} \times \boldsymbol{B}$, as described above, is the solar wind convection electric field resulting from the radially flowing (at velocity $\boldsymbol{V}_{sw}$) solar wind carrying the Parker spiral magnetic field ($\boldsymbol{B}$). These integrations, when carried out using a standard finite difference method, conserve energy to better than one part in a thousand over millions of time steps. The gyroperiod and gyroradius of an O^+ ion at 1 AU, with an assumed velocity perpendicular to the local magnetic field of 400 km s^{-1} (energy $\sim$ 13.4 keV) are $\sim$210 s and $\sim$13,400 km ($\sim 9 \times 10^{-5}$ AU), respectively. A fixed time step of 0.01 of the initial gyroperiod is used in the calculations described here. Pickup ions typically travel between 1 and 6 AU in several million time steps. The transit time of a pickup ion, because of the nature of its energization, is comparable to the transit time for solar wind plasma, or about 4 days per AU.

In the Sun-centered nonrotating frame of the present test particle calculations, both the magnetic mirror force and a form of adiabatic cooling operate. The latter is related to the invariance of magnetic flux encircled by the particle gyro-orbit as the particle moves out into the heliosphere. The magnetic mirror force, meanwhile, converts perpendicular motion to parallel motion in the diverging heliospheric magnetic field. Solar gravity generally has only a minor influence on the ion motion compared to the Lorentz force, although it can have a significant effect on the parent neutral and therefore on the pickup ion's initial velocity.

To examine the pickup ions from various sources, trajectories are calculated first for the parent neutrals, to establish the pickup ion starting positions and velocities, and then for the pickup ions themselves. Pickup ion starting points and trajectories are included only where they fall within a 6 AU heliocentric distance. While there is no inherent limit to the distance one could follow a pickup ion, scattering effects eventually become important, as does major solar wind structure not considered here such as merged interaction regions. In any case, most pickup ion observations have been made within 6 AU.

Ion production by photoionization and charge exchange by solar wind protons are to first order described by the product of the optically thin neutral source gas densities and the inverse heliocentric distance (R_{AU}) squared ion production rates. The impact ionization contribution dependence on heliocentric radius is determined by the electron temperature gradient, which is different from R_{AU}^{-2}. However, this process is rarely dominant outside the corona, except perhaps in the regions behind interplanetary shocks, and so an R_{AU}^{-2} dependence of ionization rate for pickup ion production is an often-used and generally accepted assumption. A single positive charge is assumed for all the oxygen ions traced. Finally, complications from multiple cycles of ionization and neutralization are expected to have a minor influence on the overall results on the radial scales of $R_{AU} < 6$ AU considered here. Thus, weighting of the initiation points by an inverse heliocentric distance squared factor is used to derive estimates of relative heliospheric densities from representative test particle trajectories.

Particle spatial, velocity, and angle distributions in test particle calculations are represented by the statistics of their behavior. Here those statistics are expressed as "counts," proportional to the time particles spend in a particular spatial interval in a given velocity or angle bin. This number is proportional to the ion density, the first moment of the phase-space density. A typical particle detector measures particle fluxes or intensities in specific energy and incident angle ranges. These can be related to the densities by integration over the appropriate energies, solid angle, and exposure time. The count values indicate the normalized number of time steps in a particular calculation and are not intended for direct comparisons with measurements. Rather, the shapes of the distributions are the goal of the present work. The velocity distributions are in a fixed (e.g., spacecraft) frame with respect to the Sun and are given in terms of the particle velocity $\boldsymbol{v}$ normalized by the solar wind velocity $\boldsymbol{V}_{sw}$ as in most pickup ion analyses. Pitch angles are determined from the angle between the local magnetic field and test particle velocity at each time step. Cone angles are defined as the angle between the local radial and the particle velocity.

The present strategy for examining pickup ion distribution effects begins with the calculation of sample neutral O atom trajectories from an assumed pickup ion source, during which a history of the cumulative probability of ionization and the neutral particle velocity (derived from both its source and solar gravitational forces) at each position is maintained. The incremental probabilities of ionization for each time step are calculated from the product of the ionization rates (photo-, charge exchange, and electron impact) and the time step. The neutral trajectory is terminated when the integrated ionization probability is equal to 1. This implies the probability of not having been ionized is still $1/e$ and is adopted as a conservative estimate of the closest approach of the neutral to the Sun. In a more accurate Monte Carlo–style calculation, many neutrals released in the same direction would be ionized over a range of radial distances bracketing the endpoint used here. The neutral trajectory points and velocities, together with an exponential weighting factor describing the decline of the neutral density at each position due to ionization, are then used to initiate weighted pickup ion trajectory calculations. In this

way, the statistical ion distributions obtained from the trajectories automatically include the neutral density attrition with distance from the source, and the holes carved out by ionization.

To obtain the statistical distributions (spatial, velocity, pitch-angle) of the ions as described earlier, each weighted pickup ion trajectory step is sorted into bins of heliocentric radius and longitude, normalized velocity, and local pitch and cone angles, producing contributions to each bin representing the time particles spend in it. Each trajectory is additionally weighted by the probability of ionization (proportional to inverse heliocentric distance squared) at its initiation point as it is binned.

This approach thus accounts for both the ionization effects on the neutral source cloud density and the ion production rate within the cloud. Spatial, velocity, and angle distributions calculated from the ion trajectories then give approximations to the pickup ion population characteristics for different sources. As mentioned above, the displayed statistics are arbitrarily normalized, depending on the number of neutral and ion trajectories deemed necessary to define each source pattern.

Typical values of 400 km s^{-1} for the solar wind velocity and 5 nT for the interplanetary field strength at 1 AU serve to illustrate the main points. The calculations are restricted to the heliospheric equatorial region inside 6 AU. A heliolatitude dependence of the solar wind speed would modify the calculated behavior on cones of constant heliolatitude, assuming perfectly radial flow, but the general conclusions would remain the same unless the velocity shear occurs on a scale comparable to the ion gyroradius. Similarly, the presence of the heliospheric current sheet would modify the trajectories of the test particle pickup ions within a few gyroradii of the current sheet, but this detail is neglected under the assumption that the pickup ion source plays the dominant role in determining latitudinal (or longitudinal) dependence. Scattering by magnetic field fluctuations (e.g., Giacalone et al. 2000) is also not included, since the focus here is on the underlying control by the average electric and magnetic field geometry. Such scattering will broaden the angle distributions and modify the velocity distributions and spatial distributions of the pickup ions, but if the scattering mean free path is as large as estimated from pickup ion observations (scale of an AU), the influence of the average fields should be important in the inner heliosphere.

The main questions that can be directly investigated using the test particle approach concern the effects of the heliospheric location of pickup ion birth, and of the parent neutral particle velocity. Both of these depend on the neutral source, which may be centered on a moving body (e.g., a comet or planet), circumsolar (e.g., interplanetary dust), or inflowing, such as the interstellar gas. Below, simplified descriptions of these sources are used to initiate statistical test particle pickup ion calculations toward better understanding the source signatures in observations. However, some basic insights can first be obtained from the behavior of single test particles in a radial solar wind with a Parker spiral field.

3. RESULTS

3.1. *Effects of Heliocentric Radius of Ion Creation*

The heliocentric radius at the point of creation of a pickup ion by photoionization, charge exchange with a solar wind proton, or impact ionization by solar wind electrons determines the important initial angle between $\boldsymbol{V}_{sw}$ and $\boldsymbol{B}$. This angle dictates both the magnitude of the $\boldsymbol{E} = -\boldsymbol{V}_{sw} \times \boldsymbol{B}$ electric field experienced by the ion when it is picked up and the result of the combined mirror force and electric field on the ion's initial motion. A pickup ion starting from rest exhibits the standard textbook $\boldsymbol{E} \times \boldsymbol{B}$ drift. As illustrated in Figure 1, if $\boldsymbol{V}_{sw}$ and $\boldsymbol{B}$ are perpendicular, the ion velocity oscillates between zero and the well-known $2\boldsymbol{V}_{sw}$ limit. The gyrocenter of the cycloid in this case moves at $\boldsymbol{V}_{sw}$, or equivalently, the particle undergoes purely gyrational motion in the frame moving at $\boldsymbol{V}_{sw}$. An initial velocity of the ion (from the parent neutral particle) with a component perpendicular to $\boldsymbol{B}$ turns the cycloid into a spiral with loops at the cusps or flattens out the cycloid, depending on its direction and magnitude relative to the background plasma velocity. The ion's gyrocenter travels perpendicular to $\boldsymbol{B}$ at the plasma velocity perpendicular component speed, while the original neutral's perpendicular speed is turned into gyromotion. The gyrocenter moves parallel to $\boldsymbol{B}$ at the neutral's parallel velocity.

In the inner heliosphere where $\boldsymbol{V}_{sw}$ and $\boldsymbol{B}$ are not perpendicular, this simple picture is modified. If the ion starts from rest, its initial ion maximum speed is determined by the component of $\boldsymbol{V}_{sw}$ perpendicular to $\boldsymbol{B}$, which is small close to the Sun. As the mirror force and electric field propel the particle outward, the ion experiences a spatially varying $\boldsymbol{B}$ and $\boldsymbol{E}$ that subsequently modify its initial motion. Hence, a pickup ion travels only radially into the heliosphere if it starts from rest at a location where $\boldsymbol{V}_{sw}$ and $\boldsymbol{B}$ are perpendicular. The canonical picture of pickup ion radial motion and a maximum speed of $2\boldsymbol{V}_{sw}$ strictly applies only if the ion is born in the outer solar system, where the Parker spiral angle approaches 90°.

Figure 2 illustrates trajectories of single ions launched with zero initial velocity at 0.3, 1.0, and 3.0 AU heliocentric radius in the Parker spiral field with the radial solar wind flow described above. The plots show how the ions move both near their initial pickup sites and in the larger perspective. The close-in trajectories exhibit the expected cycloidal motion for ion pickup, where the amplitudes of the cycloids depend on the magnitude of the solar wind velocity component perpendicular to the local magnetic field. On a heliospheric scale, the equatorial projections in the bottom right panel show the ions picked up at large radial distances moving nearly radially (along the x-axis here), while the ions

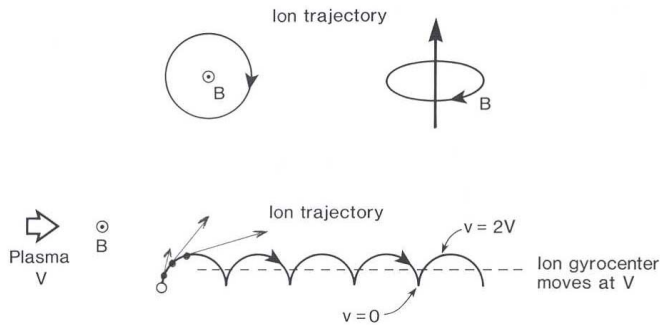

FIG. 1.—Illustration of the classical picture of ion pickup in perpendicular electric ($\boldsymbol{E} = -\boldsymbol{V}_{sw} \times \boldsymbol{B}$) and magnetic ($\boldsymbol{B}$) fields. Ions moving on the cycloidal trajectory oscillate between zero and $2\boldsymbol{V}_{sw}$ velocities, while the gyrocenter moves at $\boldsymbol{V}_{sw}$. The ion in this case is initially at rest.

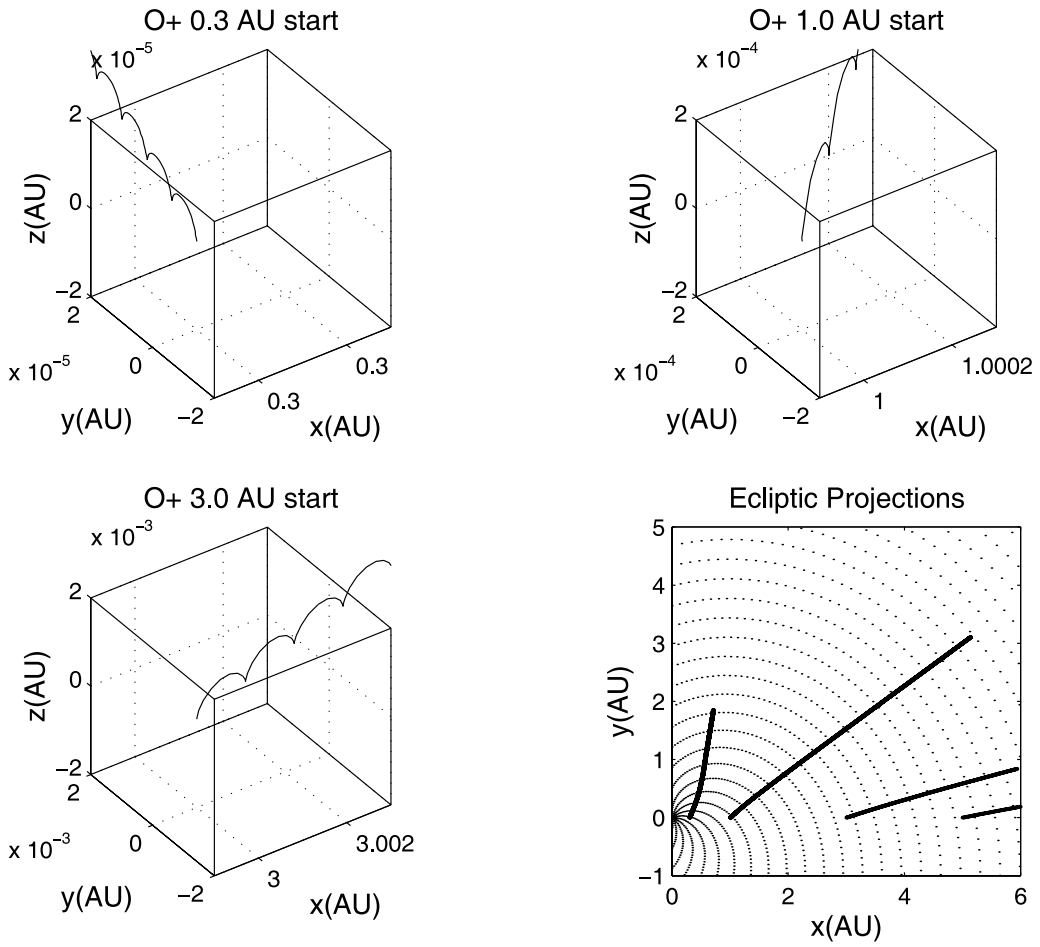

FIG. 2.—Three sample O^+ pickup ion trajectories launched at 0.3, 1.0, and 3.0 AU in a Parker spiral magnetic field and radially flowing solar wind–related convection electric field. The three-dimensional displays show their trajectories close to their points of initiation. Note the different scales. The Sun is at the origin. A larger view of the three ion trajectories, projected on equatorial Parker spiral field lines (*dotted lines*), is on the lower right. A segment for an ion launched at 5.0 AU is also included. The ion picked up at 0.3 AU moves nearly orthogonal to the radial direction inside of 1 AU and has the smallest gyroradius because the magnetic field at 0.3 AU is strongest and the convection electric field is smallest. Fig. 3 shows the velocity histories for these ions.

picked up close to the Sun initially travel nearly perpendicular to the radial through their initiation site. The picked-up ions ultimately attain a velocity consistent with the time-integrated Lorentz force experienced along their trajectories. These test particle velocity histories are shown in Figure 3, which plots only samples (~every 1000th point) from each trajectory. In the case of pickup at a radius where the Parker spiral angle (the angle between $\boldsymbol{V}_{sw}$ and $\boldsymbol{B}$) is small, this asymptotic velocity is the solar wind velocity. In the case of nearly perpendicular $\boldsymbol{V}_{sw}$ and $\boldsymbol{B}$ at pickup sites at larger heliocentric distances, the velocity range approaches the classical pickup ion values of zero to $2\boldsymbol{V}_{sw}$.

3.2. *Effects of Initial Particle Velocity*

The above-mentioned figures illustrate the difference between the heliospheric field control of pickup ions and other energetic particles such as solar energetic particles from the low corona. The initial ion velocity, whether derived from the parent neutral or from another ion acceleration process, exerts an important influence on the effect of the solar wind. Figure 4 illustrates this with the projected trajectories of ions initiated near the Sun with radial velocities 0, 400, 800, 1500, and 2000 km s^{-1}. The ion that moves perpendicular to the magnetic field is the one started from rest, like the canonical pickup ion. The 400 km s^{-1} ion continues moving radially outward at 400 km s^{-1} because it experiences no Lorentz force, while the more energetic ions increasingly follow the Parker spiral magnetic field lines. Like the latter, solar energetic particles are injected into the heliosphere with high velocities compared to solar wind speed, rendering any near-Sun convection electric field unimportant to their subsequent motion. Thus, the solar energetic particles from flares practically trace the Parker spiral magnetic field lines in a nearly field-aligned beam originating at the Sun (e.g., Giacalone et al. 2000). In contrast, the pickup ions' fates are from their creation determined by the electric field. They are dominated by the forces and drifts dictated by the radially varying Parker spiral magnetic field and the related $\boldsymbol{E} = -\boldsymbol{V}_{sw} \times \boldsymbol{B}$ convection electric field.

The effects of initial velocities from the parent neutrals also depend on the direction of those velocities as well as their magnitude. The initial velocity direction is determined in part by the nature of the neutrals' source and in part by solar gravity's effect on the neutrals. Figure 5 shows the

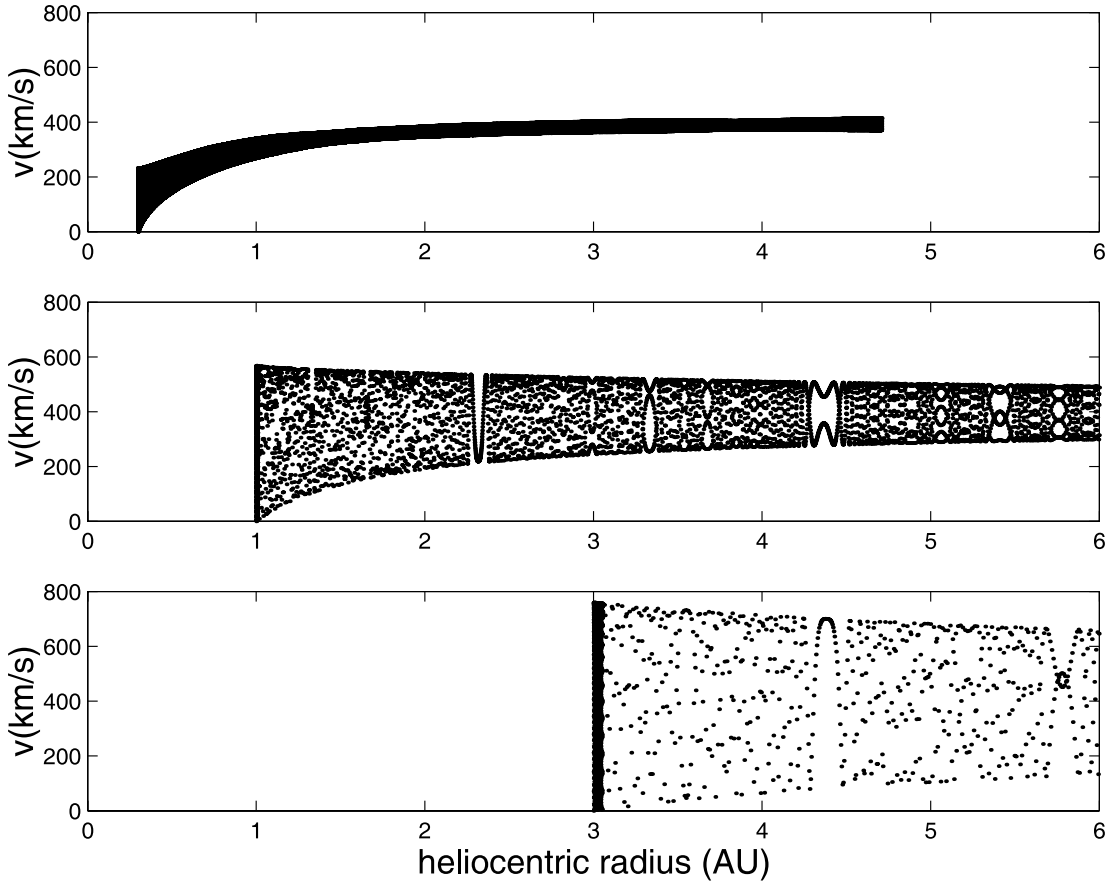

FIG. 3.—Velocity histories for the pickup O^+ ions in Fig. 2. Approximately every 1000th time step in the calculation is plotted to give an idea of their individual range of velocity and its evolution. The 0.3 AU launch point case record (*top*) is terminated early because its behavior has reached an asymptotic state where its velocities are always close to V_{sw}. This ion never exhibits the classical zero to $2V_{sw}$ velocity range. The ion launched at 1.0 AU (*middle*) more closely approaches the ideal but is still short of the classical range. The ion launched at 3.0 AU (*bottom*), where the Parker spiral angle is most nearly perpendicular, exhibits an approximately classical pickup ion velocity range. All of the velocity histories exhibit the "cooling" with radius expected for pickup ions. The occasional dot patterns result from the aliasing of the trajectory sampling.

results of launching ions with several initial velocities directed toward and away from the Sun and azimuthally in both directions. The initial velocities of 20 and 70 km s^{-1} were selected because they approximate interstellar and Jovian source examples. The results for 0.3, 1.0, and 3.0 AU initiation points in Figure 5 illustrate the degree of spread in the ion trajectories that is introduced by initial velocities of these magnitudes. The magnitudes of the effects shown do not drastically alter the overall trends of the ion behavior but could provide additional information on the pickup ions' source if distinguished in measurements.

Also important from an observational standpoint is the fact that the velocity range of the picked-up ions extends from the nonzero neutral velocity to the sum of the maximum pickup velocity (for the zero initial velocity case) plus the neutral velocity. Mobius et al. (1999) recently detected the interstellar gas velocity enhancement in the upper cutoff of the observed helium pickup ion distribution. Detecting the nonzero low-velocity cutoff requires detector capabilities not yet available.

3.3. *Effects of Initial Spatial Distributions*

The pickup ion distributions at any point reflect the radial integration of the pickup ion production and transport interior to that point (which may vary with heliolongitude and latitude as well as time, if the neutral source moves or solar EUV and solar wind conditions change). This makes the interpretation of pickup ion observations a complicated problem, especially considering the long time integrations required to measure sufficient particles to obtain a distribution. However, idealized examples that have their basis in nature give an idea of how the source properties can be inferred from test particles. For example, the interplanetary dust cloud is roughly longitudinally symmetric but radially extended and is concentrated at low heliolatitudes. The ion production near the ecliptic can thus be approximated as a function of radius only. The major ionization rates have an R_{AU}^{-2} falloff, and the neutral particle density radial profile, which for dust goes as $\sim 1/R_{AU}$, provides the ion trajectory weights for determining the related pickup ion properties. The dust disk neutrals presumably move with azimuthal Keplerian velocities. In the case of an interstellar source, a uniform flow toward the Sun from one direction at a velocity of $\sim$20–25 km s^{-1} is an appropriate description. The same inverse R^2 ion production rate multiplier can be applied to an assumed uniform density stream. However, because the gas inflow geometry produces an azimuthally as well as latitudinally asymmetric ion source, the resulting pickup ion spatial distribution also depends on

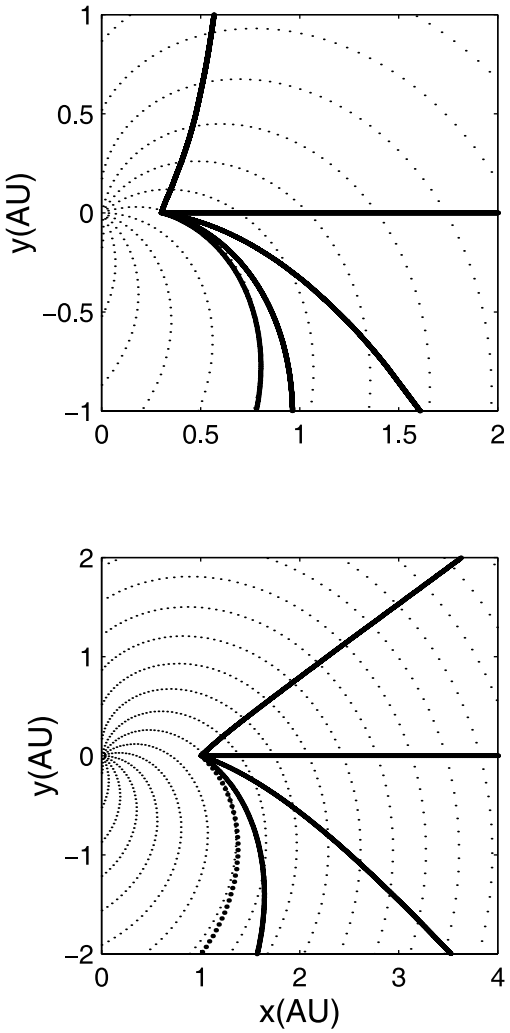

FIG. 4.—Four O^+ pickup ions launched with different initial radial velocities, 0, 400, 800, 1500, and 2000 km s^{-1}, at 0.3 AU (*top*) and 1.0 AU (*bottom*) starting points on the *x*-axis. The ion picked up from rest moves across the Parker spiral field. The 400 km s^{-1} ion moves radially at 400 km s^{-1} because it experiences no force. The faster particles move increasingly along the spiral magnetic field.

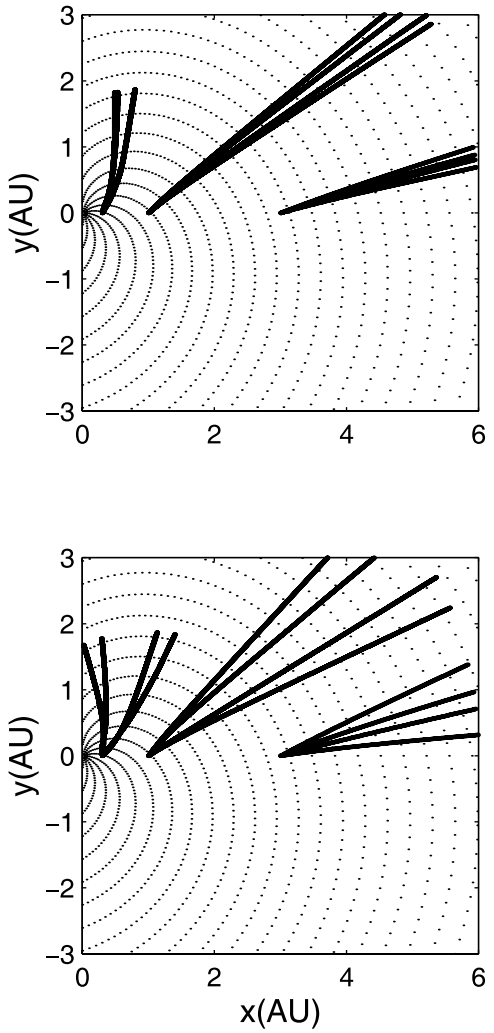

FIG. 5.—Trajectories of an O^+ ion launched with 20 km s^{-1} (*top*) and 70 km s^{-1} (*bottom*) initial velocities at 0.3, 1.0, and 3.0 AU in four orthogonal directions in the equatorial plane. The spread of the trajectories indicates the effect of initial velocity magnitude and direction for several reasonable values of parent neutral velocity.

heliolongitude in the equatorial plane. Moreover, the interstellar neutral source density has a circumsolar hole carved out by solar ionization.

For a localized source like a comet or planet, the assumption of a neutral source outflow at a specific velocity approximately describes the situation. Again, even with a purely radially dependent ion production rate, the pickup ion source has heliolatitude and -longitude dependences, but they differ from those for the interstellar gas inflow or dust disk source. Moreover, in these cases the source may move on a timescale that is significant compared to the pickup ion transit times over AU distances, introducing a structure into the neutral source's spatial distribution (e.g., Luhmann 1994). An additional consideration is that the localized source neutral velocities may not be sufficient to spread the neutrals spatially before they are ionized. Under such circumstances, the pickup ions are almost all produced near the source, where they mass-load and alter the plasma flow and field responsible for ion pickup. The effect of local field draping due to either mass-loading or the presence of an obstacle (e.g., a magnetosphere or an ionosphere) in the region of ion pickup will tend to promote perpendicular pickup geometries. Low initial pickup velocities also result if there are mass-loading or magnetosheath flow stagnation effects. Consideration of these details in the vicinity of localized sources is beyond the scope of the present analysis. In any case, several earlier studies (e.g., Luhmann, Fedder, & Winske 1988; Kallio & Koskinen 1999) already considered the properties of test particle pickup ions in the vicinities of comets and unmagnetized planets. The Jovian case described earlier by Luhmann (1994, 2003), based on the assumption of an Io torus source producing an extended cloud of ~75 km s^{-1} O in the heliosphere, is reexamined here for comparison purposes.

Figures 6–8 display the results for three hypothetical oxygen sources, including interstellar gas inflow (Figs. 6*a*–6*f*), a Keplerian circumsolar disk representing an interplanetary dust–related oxygen source (Figs. 7*a*–7*f*), and a Jovian (Io torus) source (Figs. 8*a*–8*f*). The interstellar medium (ISM) source case shows the focusing of the neutral trajectories by the solar gravitational field but does not produce a focusing

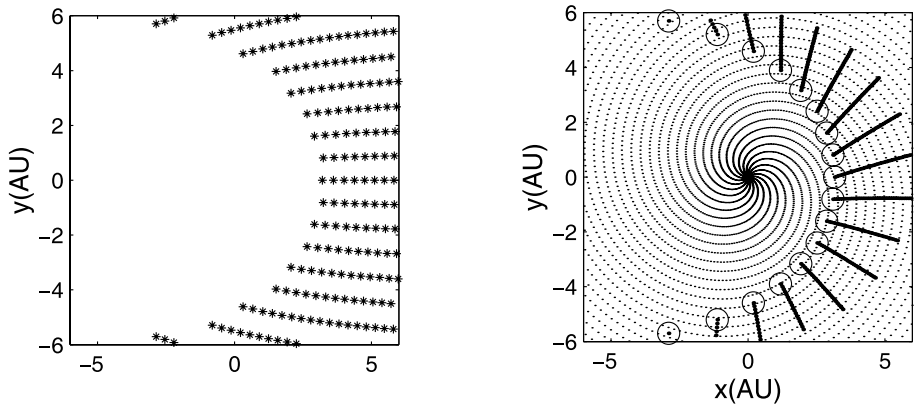

FIGS. 6*a* AND 6*b*

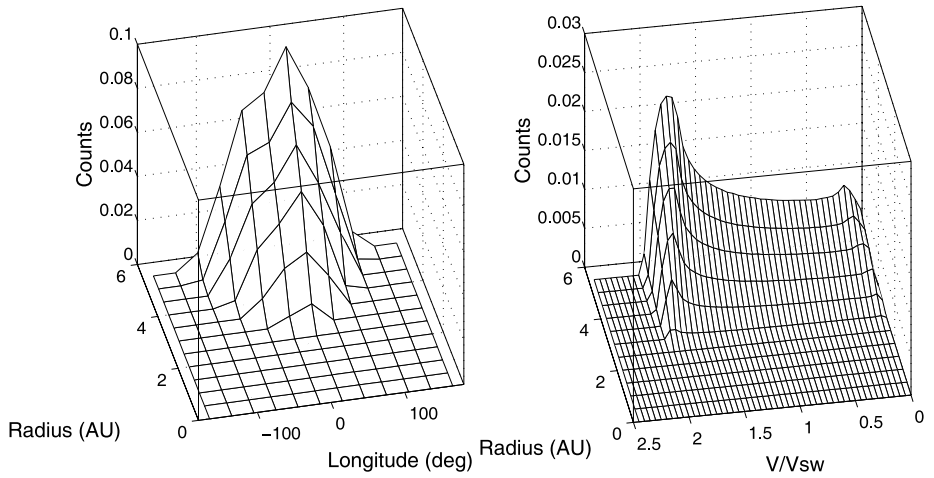

FIGS. 6*c* AND 6*d*

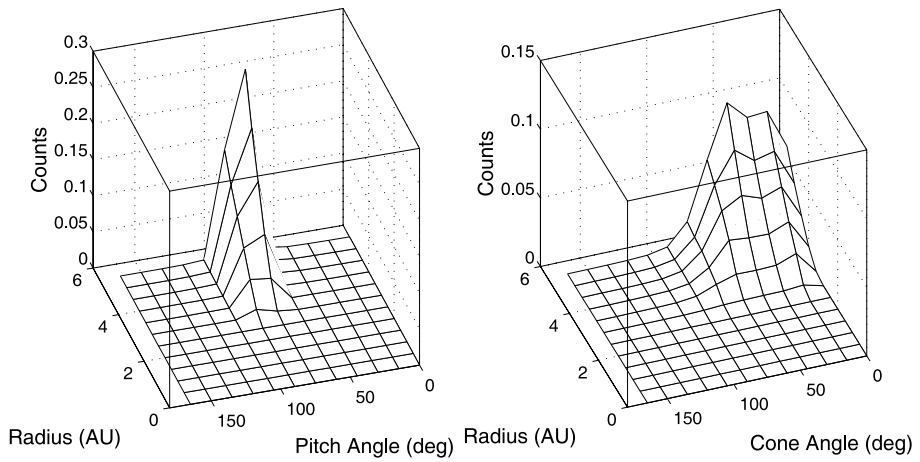

FIGS. 6*e* AND 6*f*

FIG. 6.—Results of calculations for a hypothetical ISM source of heliospheric atomic oxygen. (*a*) Trajectories of O atoms that enter the heliosphere at 20 km s^{-1} from the right and are focused by solar gravity. They terminate where the path-integrated probability for ionization is equal to 1. The points inside 6 AU are used as starting points for calculating the statistical descriptions of the resulting pickup ions. (*b*) Sample pickup O^+ trajectories projected on the solar equatorial plane, calculated using the innermost points of (*a*) as their starting points. The initial O^+ velocities are presumed to be the velocities of the parent neutrals, which are slightly altered by solar gravity. The departures of these ion trajectories from radial result from their initial velocities and the non-perpendicular V_{sw} and magnetic field at their sites of origin. The ion trajectory tracing is stopped at 6 AU. (*c*) Statistical distribution of O^+ density (proportional to "counts" by an arbitrary factor depending on the number of particles and time steps in the calculations), as a function of heliocentric radius and heliolongitude for the ISM O source. Heliolongitude is measured counterclockwise from the *x*-axis. The pickup ions are concentrated in the upstream hemisphere where the O atoms penetrate the heliosphere inside 6 AU. (*d*) Statistical velocity distribution for the pickup ions, showing a nearly classical range from small speeds to almost twice the solar wind speed, with the departures due to the 20 km s^{-1} initial velocities of the ions from the parent neutrals, as well as the modestly off-perpendicular geometry of the pickup electric fields (see [*b*]). (*e*) Statistical pitch-angle distribution for the ISM source O^+ ions as a function of heliocentric radius. The classical pickup ion peak around a 90° pitch angle is evident. (*f*) Statistical cone-angle distribution as a function of heliolongitude for the ISM O source. The cone angle is the angle between the local radial and the particle velocity.

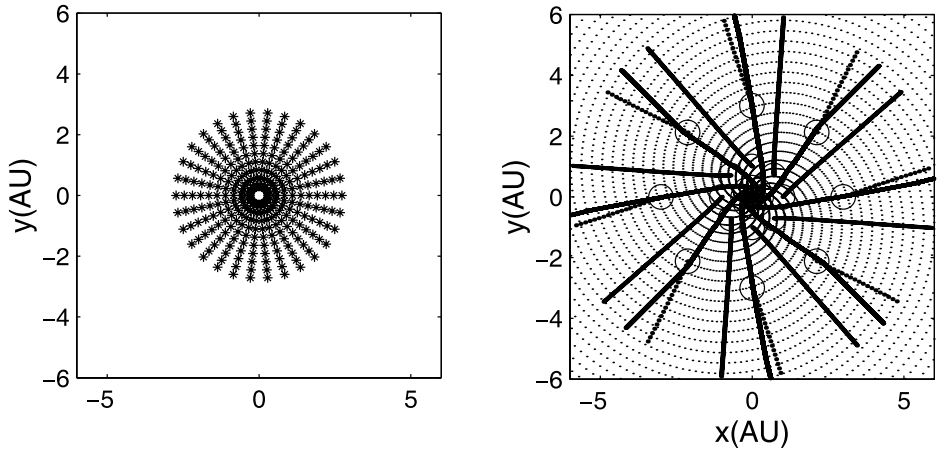

FIGS. 7*a* AND 7*b*

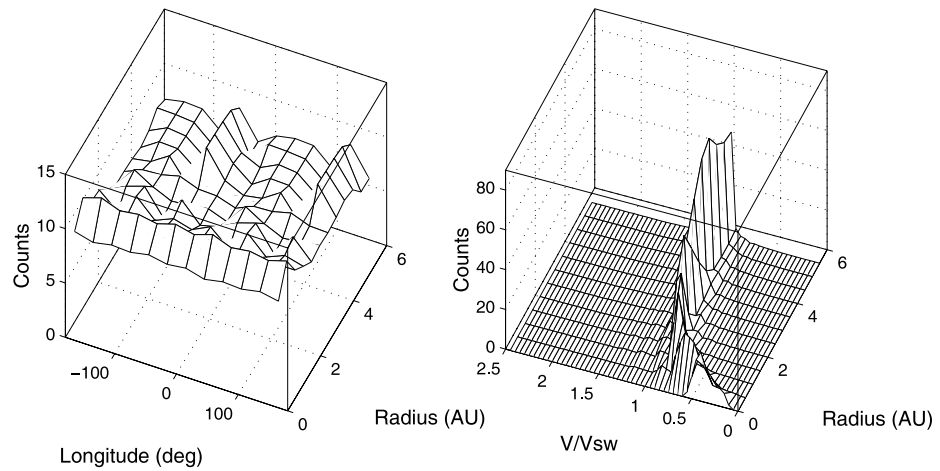

FIGS. 7*c* AND 7*d*

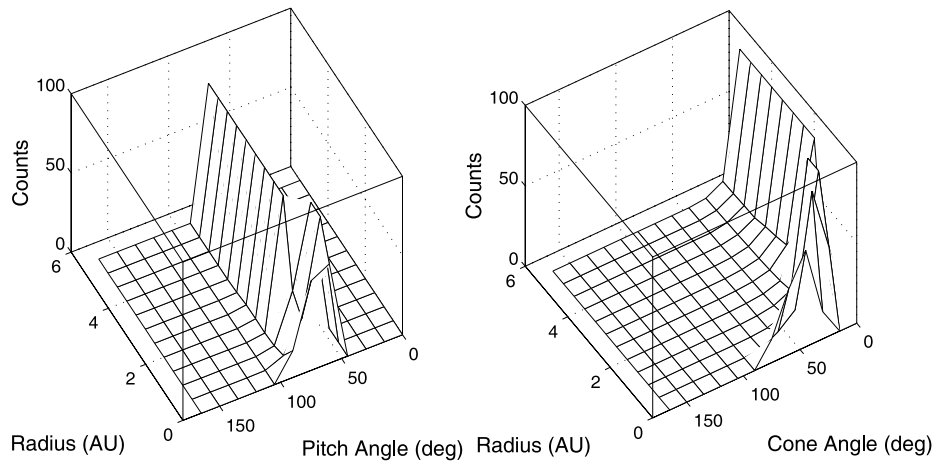

FIGS. 7*e* AND 7*f*

FIG. 7.—Same as Fig. 6, but for a Keplerian disk of neutral O source atoms distributed between 0.3 and 3.0 AU, as seen in (*a*). Note that in this case, termination of the neutral cloud by solar ionization is not an issue. The assumed neutral O density depends on the inverse heliocentric distance. The initial counterclockwise azimuthal Keplerian velocities of the related pickup ions range from 57 km s^{-1} at 0.3 AU to 17 km s^{-1} at 3.0 AU. (*b*) Sample pickup O^+ trajectories. In this case sample ion trajectories are shown for initiation at 0.3, 1.0, and 3.0 AU heliocentric rings. The ions launched from the innermost ring show the nonradial motion expected from the earlier single-particle tests. (*c*) O^+ spatial distribution for this source is approximately flat except for fluctuations due to the limited test particle statistics and the bin sizes and locations. (*d*) Velocity distributions for the source are strikingly different than for the ISM source in Fig. 6. Because ions produced in the inner ring dominate due to the falloff of the starting point density with radius (see top panel of Fig. 5) and the inverse radius squared dependence of the ion production rate, the O^+ from this source is dominated by particles picked up at small Parker spiral angles. Thus, their statistical behavior reflects the test case velocities in the top panel of Fig. 3. (*e*) Pitch-angle distribution again peaks at 90° after a start-up period of adjustment in the nonperpendicular field and solar wind flow conditions in the inner disk. (*f*) Cone-angle distribution shows an evolution in the inner heliosphere due to the initially perpendicular (to the radial) motion of inner disk pickup ions (see [*b*]).

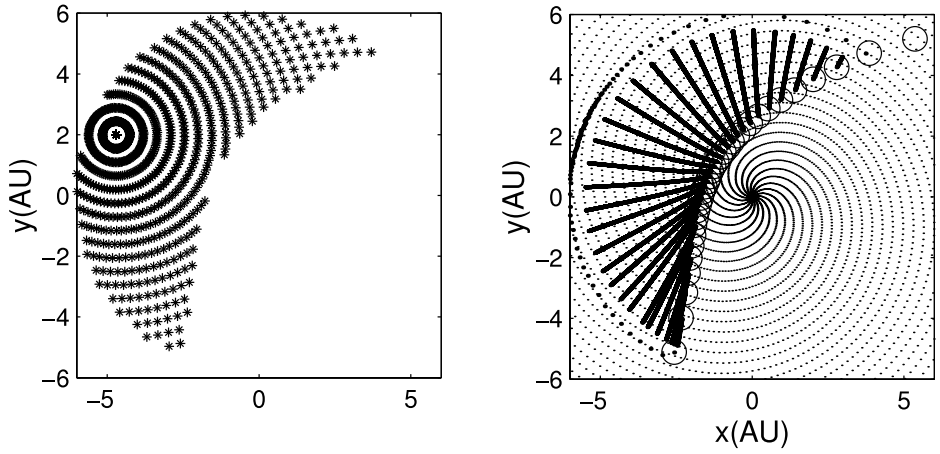

FIGS. 8*a* AND 8*b*

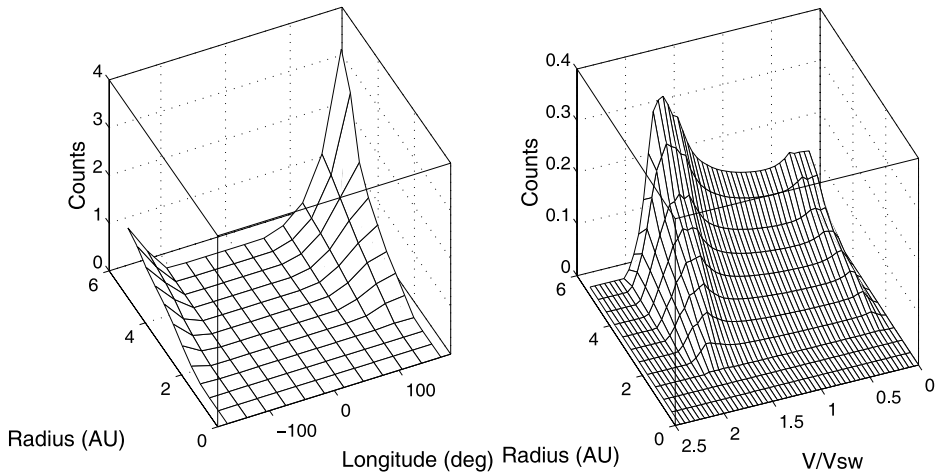

FIGS. 8*c* AND 8*d*

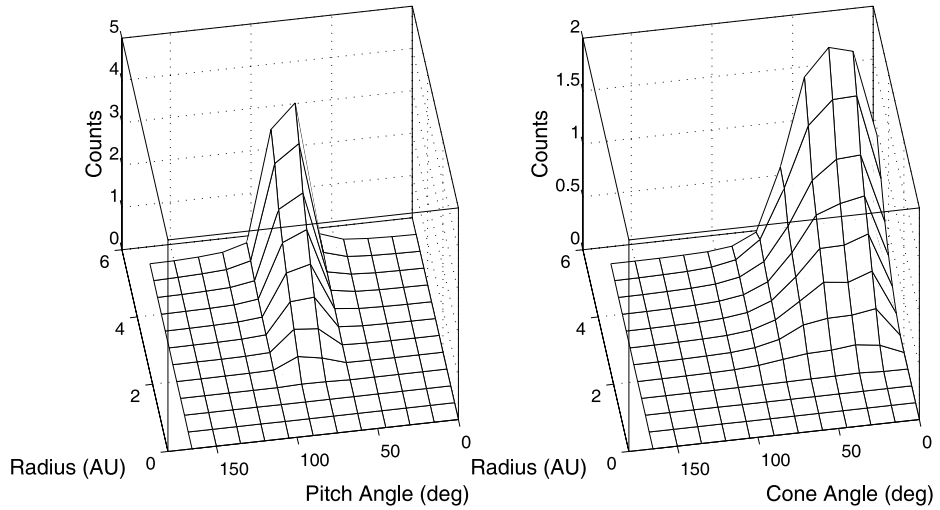

FIGS. 8*e* AND 8*f*

FIG. 8.—(*a*) Same as Figs. 6 and 7, but for a Jovian torus source of neutral O. This case more closely resembles the ISM case in Fig. 6 because the neutrals approach the Sun from a distance, and ionization limits their closest approach. However, the ~75 km s^{-1} velocities of the neutrals emitted from Jupiter's location are more significant compared to the solar wind speed, allowing the neutrals to reach smaller heliocentric distances than in the ISM case (Fig. 6*a*). (*b*) Sample pickup O^+ trajectories. The ions show the effect of the initial neutral velocities for this source moving along Jupiter's orbit at ~13 km s^{-1}. (*c*) Spatial distribution is more closely concentrated around a single radial since Jupiter is an effective point source of neutrals at ~5 AU. (*d*) O^+ pickup ions' velocity distribution has a noticeably nonzero lower limit and generally narrower appearance than that in Fig. 6*d*. The difference at low velocity is due to both the 75 km s^{-1} minimum velocity of these pickup ions, derived from their parent neutrals, and the smaller Parker spiral angle at the sites of Jovian ion production close to the Sun (see [*b*]). The initial velocities of some of these pickup ions are in fact increased by solar gravity to ~90 km s^{-1}. (*e, f*) Pitch-angle and cone-angle distributions for the Jovian source resemble those for the interstellar source in Figs. 6*e*–6*f* because of the similar spread in the pickup ion starting point distribution.

cone inside 6 AU for the moderately quiet-Sun photoionization rate used of 2.5×10^{-7} s^{-1}. The ISM neutrals are presumed to enter the heliosphere from the right in Figure 6*a*, in a uniform stream moving at ~20 km s^{-1}. The Keplerian disk neutral source in Figure 7*a* was presumed located in the radial range 0.3–3.0 AU, with a $\sim 1/R_{AU}$ dependence in starting point density and initial azimuthal Keplerian velocities. The Jovian source in Figure 8*a*, like those described in previous publications (Luhmann 1994, 2003), is represented by a point source at the ~5 AU heliocentric distance of Jupiter, moving at ~13 km s^{-1} along Jupiter's orbit and emitting neutrals at ~75 km s^{-1} (the corotation velocity at Io's orbit) relative to Jupiter. Equatorial projections of the neutral O trajectories are first shown for each source, together with sample pickup ion trajectories for the starting points (Figs. 6*b*, 7*b*, and 8*b*). For the statistical calculations, all of the neutral trajectory points shown are used as starting points for pickup ion trajectories. The heliocentric radius versus longitude gradients in the pickup ion density and the radial gradients in the calculated ion velocity, pitch-angle, and cone-angle distributions are displayed in Figures 6*c*–6*f*, 7*c*–7*f*, and 8*c*–8*f*.

The roots of the differences in the statistical spatial distributions for the pickup ions can be readily understood from the starting point distributions and sample pickup ion trajectories in Figures 6*a*–6*b*, 7*a*–7*b*, and 8*a*–8*b*. The spatial distributions in Figures 6*c*, 7*c*, and 8*c* result from the combination of the inverse heliocentric distance squared weighting of the ion trajectories and the distribution of the ion starting points (Figs. 6*a*, 7*a*, and 8*a*). The particular Jovian source description used here makes a more narrowly confined longitude distribution of O^+ pickup ion density than the ISM source. The disk source density distribution is uniform in heliolongitude (with some fluctuations from the small statistics).

The differences in the radially dependent ion velocity distributions in Figures 6*d*, 7*d*, and 8*d* reflect the initial pickup electric field and mirror force effects. For example, for the Keplerian disk source from 0.3 to 3.0 AU shown in Figures 7*a*–7*b*, the velocity distribution in Figure 7*d* starts out fairly broad, although reaching less than $\boldsymbol{V}_{sw}$, and is sharply peaked at the solar wind velocity by about 4 AU. If the inner radius of the disk had been at ~5 AU, the ion velocity distributions would have been more classical, spanning the velocity range from zero to $2\boldsymbol{V}_{sw}$, due to the more nearly perpendicular $\boldsymbol{V}_{sw}$ and $\boldsymbol{B}$ geometry at the ion initiation sites. The effects of a significant initial velocity of the parent neutral can appear as shifts from the classical zero-velocity initial pickup behavior and shifts in the maximum $2\boldsymbol{V}_{sw}$ velocity, but these effects can be masked by contributions from a radially extended source when the source is strong at smaller Parker spiral angles, as in this case. The velocity distributions for the interstellar gas source in Figure 6*d* and the Jovian source in Figure 8*d* are relatively classical in their appearance. The primary exception is that the Jovian distribution exhibits a narrower spread because of the sunward 75 km s^{-1} minimum velocities gained from the parent neutrals, compared to the 20 km s^{-1} minimum velocities in the interstellar source case. Figure 9 displays the velocity distributions in Figures 6*c*, 7*c*, and 8*c* projected along their radial axes to emphasize the differences and to suggest the implications of a lack of radial gradient information in the case of the Keplerian disk source.

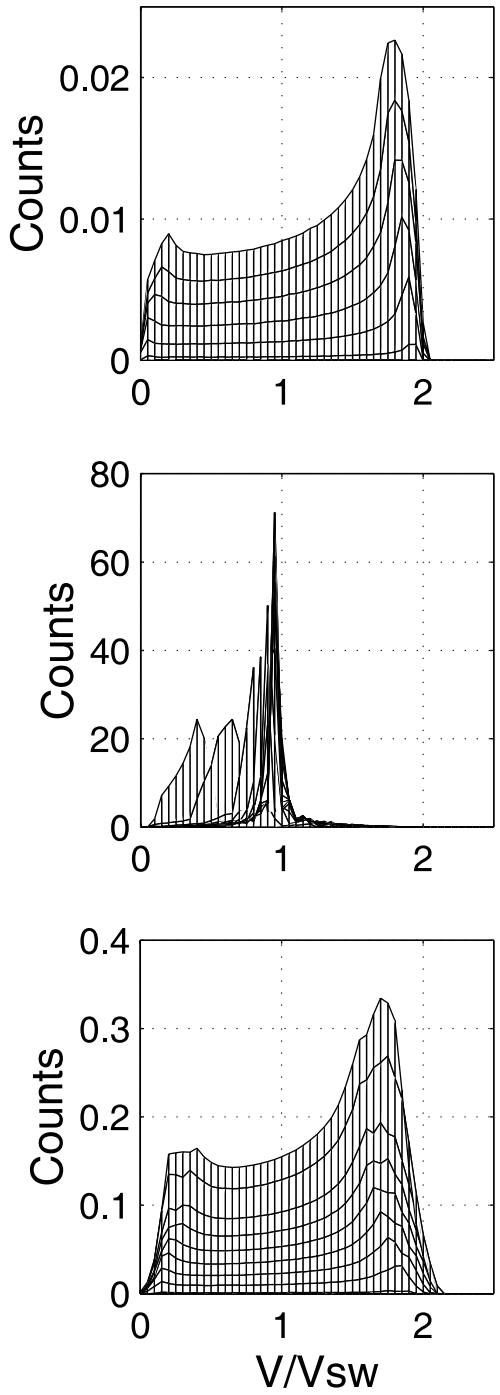

FIG. 9.—Comparison of velocity distributions in Figs. 6*c*, 7*c*, and 8*c* (*top, middle, and bottom, respectively*), projected along their radial axis to emphasize the comparisons when radial gradient information is suppressed. These views also better show the differences in the interstellar and Jovian ion velocity distributions from the 20 and 75 km s^{-1} parent neutral velocity differences.

In all cases, the pitch-angle distributions in Figures 6*e*, 7*e*, and 8*e* exhibit the expected pickup ion peaks at 90° following initial adjustments near the pickup site. Had the initial ion (e.g., the parent neutral) velocities been field-aligned and large compared to the solar wind speed, as for the high-velocity cases in Figure 4, the pitch-angle distribution would have been less perpendicular. The cone-angle distributions are more interesting in that the Keplerian disk case in

Figure 7*f* shows a radial evolution related to the stronger Keplerian neutral velocity in the inner disk. However, farther out in the heliosphere the disk source produces a much more narrowly confined cone-angle distribution compared to the interstellar and Jovian source cases in Figures 6*f* and 8*f*. The reason the latter are broader is seen in the sample ion trajectories in Figures 6*b* and 8*b* and the neutral starting point distributions in Figures 6*a* and 8*a*. Many of the ions are picked up where the initial (parent neutral) velocity is roughly along the direction of the local magnetic field. It takes a long time for these particles to be turned around and carried outward (e.g., see the point densities in the bottom panel of Fig. 3), and so off-radial cone angles contribute substantially to the densities. Of course, in the real case there would be more variations in the initial velocity magnitudes and directions in the Keplerian disk, so that this contrast would not be as noticeable as suggested by these calculations. Observations of the combined characteristics in the full set of figures for each source would help to provide a definitive source identification for a pickup ion population.

4. DISCUSSION AND CONCLUSIONS

Although the calculations described here are simple in concept compared to the transport equation–based approaches to describing the behavior of pickup ions and neglect the effects of diffusive processes in the scatter-free limit chosen, they provide some unique information. In particular, the results suggest how features of the spatial and velocity distributions of pickup ions can be interpreted in terms of heliospheric-scale field configurations, source distributions, and ionization processes that underlie any diffusive processes. Especially on the scale of the heliosphere inside of $\sim$6 AU, the neglect of scattering may not be a severe shortcoming. The ions must in any case respond to the average heliospheric fields, including those at their sites of origin, which here largely determine their spatial and velocity distributions throughout the heliosphere.

As mentioned in the introduction, solar energetic protons in impulsive (flare-related) events have been successfully modeled as test particles, albeit with some weak scattering processes included (Giacalone et al. 2000). The first-order behavior of these energetic protons is their average streaming motion along the Parker spiral magnetic field. Pickup ions, especially heavier ions with large gyroradii such as O^+, arguably follow the same rules, except that they start with zero to modest velocities in regions where they are greatly affected by the solar wind convection electric field. Scattering algorithms can readily be added to calculations such as those described here, but the gross conclusions concerning the ions' average behavior should not be affected.

The present results suggest some observational tests that could be done to further examine the question of pickup ion sources. Upstream and downstream asymmetries in the densities of the interstellar helium pickup ions have already been detected by Mobius et al. (1999), but the heliolongitude distribution of pickup O^+ ions has not yet been revealed. A Keplerian disk source population would show no heliolongitude asymmetry, thus clearly identifying it. These two proposed sources for O^+ have already been found to exhibit distinctive velocity distributions (e.g., Gloeckler et al. 2000) resembling those found here. The Jovian torus source ion distribution would, of course, move with Jupiter and show velocity cutoffs consistent with the expected initial velocities of $\sim$75 km s^{-1}. The cone-angle distributions derived from the above calculations suggest an additional analysis that may be worthwhile. Most important, the test particle approach provides the capability of examining complicated source scenarios and features that would be extremely difficult to handle with transport equation methods. The two approaches together provide a complementary combination of tools for exploring the many nuances of pickup ions in the heliosphere.

Support for this work was provided by NASA subaward F006454 as part of the Cassini INMS Investigation.

REFERENCES

Barbosa, D. D., Eviatar, A., & Siscoe, G. L. 1984, J. Geophys. Res., 89, 3789
Fichtner, H., le Roux, J. A., Mall, U., & Rucinski, D. 1996, A&A, 314, 650
Giacalone, J., Jokipii, J. R., & Mazur, J. E. 2000, ApJ, 532, L75
Gloeckler, G., Fisk, L. A., & Schwadron, N. 1995, Geophys. Res. Lett., 24, 93
Gloeckler, G., Fisk, L. A., Zurbuchen, T. H., & Schwadron, N. A. 2000, in AIP Conf. Proc. 528, Acceleration and Transport of Energetic Particles Observed in the Heliosphere: ACE-2000 Symposium, ed. R. A. Mewaldt (Melville: AIP), 221
Isenberg, P. A. 1997, J. Geophys. Res., 102, 4719
Kallenbach, R., Geiss, J., Gloeckler, G., & von Steiger, R. 2000, Ap&SS, 274, 97
Kallio, E., & Koskinen, H. 1999, J. Geophys. Res., 104, 557
Krimigis, S. M., et al. 2002, Nature, 415, 994
Lu, J. Y., & Zank, G. P. 2001, J. Geophys. Res., 106, 5709
Luhmann, J. G. 1994, J. Geophys. Res., 99, 13285
———. 2003, Planet. Space Sci., in press
Luhmann, J. G., Fedder, J. A., & Winske, D. 1988, J. Geophys. Res., 93, 7532
Mobius, E., et al. 1985, Nature, 318, 426
———. 1999, Geophys. Res. Lett., 26, 3181
Neugebauer, M. 1990, Rev. Geophys., 28, 231
Vasyliunas, V., & Siscoe, G. L. 1976, J. Geophys. Res., 81, 1247